

Hybrid high-order methods for the numerical simulation of elasto-acoustic wave propagation



Romain Mottier^{§†‡}

Alexandre Ern^{†‡} and Laurent Guillot[§]

WCCM/PANACM, Vancouver – Canada, 21-26 July 2024,

[§] CEA, DAM, DIF, F-91297 Arpajon, France

[†] CERMICS, Ecole des Ponts, F-77455 Marne la Vallée cedex 2

[‡] SERENA Project-Team, INRIA Paris, F-75647 Paris France

Table of Contents

1 Introduction

- Context
- DG and HHO methods
- Model Problem

2 RK-HHO discretization

- HHO space semi-discretization
- Singly diagonally implicit RK schemes
- Explicit RK schemes

3 Numerical results

- Convergence rates
- CFL stability condition
- Ricker wavelet
- Sedimentary basin

Table of Contents

1 Introduction

- Context
- DG and HHO methods
- Model Problem

2 RK-HHO discretization

- HHO space semi-discretization
- Singly diagonally implicit RK schemes
- Explicit RK schemes

3 Numerical results

- Convergence rates
- CFL stability condition
- Ricker wavelet
- Sedimentary basin

Goal

- Accurate simulation of seismo-acoustic waves through **heterogeneous domains with complex geometries**

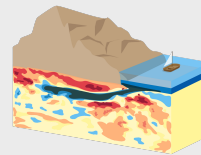
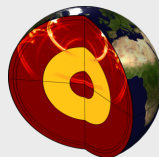


Fig. 1: Global seismic wave propagation

Fig. 2: Local heterogeneities of the Earth

- Minimize numerical dispersion and dissipation for long time propagation

Goal

- Accurate simulation of seismo-acoustic waves through **heterogeneous domains with complex geometries**

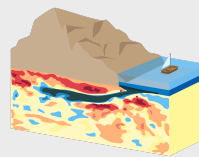
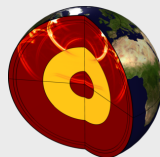


Fig. 1: Global seismic wave propagation

Fig. 2: Local heterogeneities of the Earth

- Minimize numerical dispersion and dissipation for long time propagation

Commonly used numerical tools

- Spectral Element Method (cG) / Finite Differences (FD)

Goal

- Accurate simulation of seismo-acoustic waves through **heterogeneous domains with complex geometries**

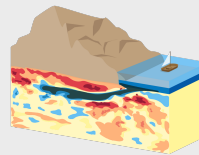
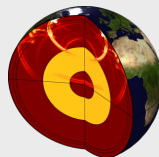


Fig. 1: Global seismic wave propagation

Fig. 2: Local heterogeneities of the Earth

- Minimize numerical dispersion and dissipation for long time propagation

Commonly used numerical tools

- Spectral Element Method (cG) / Finite Differences (FD)
- **Main issue:** Complex mesh generation for realistic geological structures

cG vs. dG methods

Main advantages of dG methods

- **Mesh flexibility:** Handling of unstructured / polyhedral meshes
- **Local conservativity at the element level**
- **Same order of convergence as cG for smooth solutions:**
 - ▶ H^1 -error: $\mathcal{O}(h^k)$
 - ▶ L^2 -error: $\mathcal{O}(h^{k+1})$

cG vs. dG methods

Main advantages of dG methods

- **Mesh flexibility:** Handling of unstructured / polyhedral meshes
- **Local conservativity at the element level**
- **Same order of convergence as cG for smooth solutions:**
 - ▶ H^1 -error: $\mathcal{O}(h^k)$
 - ▶ L^2 -error: $\mathcal{O}(h^{k+1})$

Drawbacks of dG methods

- **Higher computational cost and memory requirement**

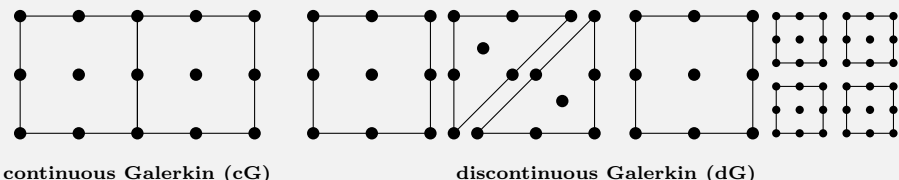


Fig. 3: Discrete unknowns for cG and dG methods

Introduction to HHO methods

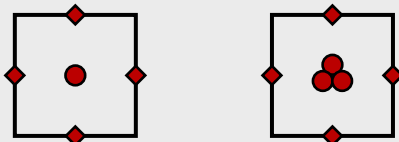
- **Seminal papers:** [Di Pietro, Ern, and Lemaire, 2014], [Di Pietro and Ern, 2015]

Introduction to HHO methods

- Seminal papers: [Di Pietro, Ern, and Lemaire, 2014], [Di Pietro and Ern, 2015]

Degrees of freedom

- Polynomial unknowns attached to mesh cells and faces



HHO local unknowns:
 $\hat{u}_T := (u_T, u_{\partial T})$

- Cell unknowns, degree $k' \in \{k, k+1\}$
- ◆ Face unknowns, degree $k \geq 0$

Fig. 4: Local HHO unknowns. **Left:** $k' = k = 0$. **Right:** $k' = k+1 = 1$.

- ▶ Equal-order: $k' = k$
- ▶ Mixed-order: $k' = k+1$

Design

■ Gradient reconstruction operator:

$$(\nabla \mathbf{u})_{|T} \rightarrow \mathbf{G}_T(\hat{\mathbf{u}}_T) \in \mathbb{P}^k(T; \mathbb{R}^d)$$

Design of $\mathbf{G}_T(\hat{\mathbf{u}}_T)$ mimics an integration by parts

■ Stabilization operator: $\boldsymbol{\delta}_{\partial T}(\hat{\mathbf{u}}_T) := \mathbf{u}_{\partial T} - \mathbf{u}_{T|\partial T} \approx \mathbf{0}$

Matching of cell dofs trace with face dofs (weakly)

Design

■ Gradient reconstruction operator:

$$(\nabla u)_{|T} \rightarrow \mathbf{G}_T(\hat{u}_T) \in \mathbb{P}^k(T; \mathbb{R}^d)$$

Design of $\mathbf{G}_T(\hat{u}_T)$ mimics an integration by parts

■ Stabilization operator: $\boldsymbol{\delta}_{\partial T}(\hat{u}_T) := \mathbf{u}_{\partial T} - \mathbf{u}_{T|\partial T} \approx \mathbf{0}$

Matching of cell dofs trace with face dofs (weakly)

Advantages of HHO over dG methods

■ Improved error estimates for smooth solutions

- ▶ H^1 -error: $\mathcal{O}(h^{k+1})$
- ▶ L^2 -error: $\mathcal{O}(h^{k+2})$

■ Attractive computational costs

Elimination of cell unknowns by **static condensation**

- ▶ Global problem couples only face dofs
- ▶ Cell dofs recovered by local post-processing

Design

■ Gradient reconstruction operator:

$$(\nabla \mathbf{u})_{|T} \rightarrow \mathbf{G}_T(\hat{\mathbf{u}}_T) \in \mathbb{P}^k(T; \mathbb{R}^d)$$

Design of $\mathbf{G}_T(\hat{\mathbf{u}}_T)$ mimics an integration by parts

■ Stabilization operator: $\boldsymbol{\delta}_{\partial T}(\hat{\mathbf{u}}_T) := \mathbf{u}_{\partial T} - \mathbf{u}_{T|\partial T} \approx \mathbf{0}$

Matching of cell dofs trace with face dofs (weakly)

Advantages of HHO over dG methods

■ Improved error estimates for smooth solutions

- ▶ H^1 -error: $\mathcal{O}(h^{k+1})$
- ▶ L^2 -error: $\mathcal{O}(h^{k+2})$

■ Attractive computational costs

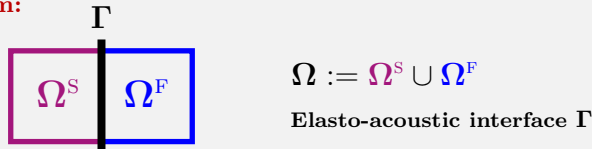
Elimination of cell unknowns by **static condensation**

- ▶ Global problem couples only face dofs
- ▶ Cell dofs recovered by local post-processing

Link to other methods

$$\text{HHO} \equiv \text{HDG} \equiv \text{WG} \equiv \text{ncVEM}$$

[Cockburn, Di Pietro, and Ern, 2016] [Lemaire, 2020] [Cicuttin, Ern, and Pignet, 2021]

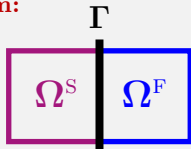
■ Model problem:

$$\Omega := \Omega^S \cup \Omega^F$$

Elasto-acoustic interface Γ

Fig. 5: Setting for elasto-acoustic coupling

■ Model problem:



$$\Omega := \Omega^S \cup \Omega^F$$

Elasto-acoustic interface Γ

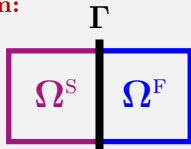
Fig. 5: Setting for elasto-acoustic coupling

Strong form of acoustic and elastic wave equation in 1st order formulation

$$\begin{cases} \partial_t \boldsymbol{\varepsilon} - \nabla_s \boldsymbol{v}^s = \mathbf{0} \\ \rho^s \partial_t \boldsymbol{v}^s - \nabla \cdot (\mathcal{C} : \boldsymbol{\varepsilon}) = \boldsymbol{f}^s \end{cases}$$

$$\begin{cases} \rho^F \partial_t \boldsymbol{v}^F - \nabla p = \mathbf{0} \\ \frac{1}{\kappa} \partial_t p - \nabla \cdot \boldsymbol{v}^F = f^F \end{cases}$$

■ Model problem:



$$\Omega := \Omega^S \cup \Omega^F$$

Elasto-acoustic interface Γ

Fig. 5: Setting for elasto-acoustic coupling

Strong form of acoustic and elastic wave equation in 1st order formulation

$$\begin{cases} \partial_t \boldsymbol{\varepsilon} - \nabla_s \boldsymbol{v}^s = \mathbf{0} \\ \rho^s \partial_t \boldsymbol{v}^s - \nabla \cdot (\mathcal{C} : \boldsymbol{\varepsilon}) = \boldsymbol{f}^s \end{cases}$$

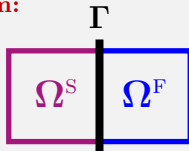
Unknowns

- \boldsymbol{v}^s elastic velocity field
- $\boldsymbol{\varepsilon} := \nabla_s \boldsymbol{u}$ linearized strain tensor

$$\begin{cases} \rho^F \partial_t \boldsymbol{v}^F - \nabla p = \mathbf{0} \\ \frac{1}{\kappa} \partial_t p - \nabla \cdot \boldsymbol{v}^F = f^F \end{cases}$$

- p scalar pressure field
- \boldsymbol{v}^F acoustic velocity field

■ Model problem:



$$\Omega := \Omega^S \cup \Omega^F$$

Elasto-acoustic interface Γ

Fig. 5: Setting for elasto-acoustic coupling

Strong form of acoustic and elastic wave equation in 1st order formulation

$$\begin{cases} \partial_t \varepsilon - \nabla_s \mathbf{v}^s = \mathbf{0} \\ \rho^s \partial_t \mathbf{v}^s - \nabla \cdot (\mathcal{C} : \varepsilon) = \mathbf{f}^s \end{cases}$$

Unknowns

$$\begin{cases} \rho^F \partial_t \mathbf{v}^F - \nabla p = \mathbf{0} \\ \frac{1}{\kappa} \partial_t p - \nabla \cdot \mathbf{v}^F = f^F \end{cases}$$

► \mathbf{v}^s elastic velocity field

► p scalar pressure field

► $\varepsilon := \nabla_s \mathbf{u}$ linearized strain tensor

► \mathbf{v}^F acoustic velocity field

Parameters

► $\rho^s, \mathcal{C}(\lambda, \mu)$ (Lamé coefficients)

► ρ^F, κ

$$\text{► } c_p^s := \sqrt{\frac{\lambda + 2\mu}{\rho^s}}, \quad c_s := \sqrt{\frac{\mu}{\rho^s}}$$

$$\text{► } c_p^F := \sqrt{\frac{\kappa}{\rho^F}}$$

Coupling conditions

$$\begin{cases} \mathbf{v}^{\text{S}} \cdot \mathbf{n}_{\Gamma} = \mathbf{v}^{\text{F}} \cdot \mathbf{n}_{\Gamma} & \blacktriangleright \text{Balance of mass + Non-penetration condition} \\ (\mathcal{C} : \boldsymbol{\varepsilon}) \cdot \mathbf{n}_{\Gamma} = p \mathbf{n}_{\Gamma} & \blacktriangleright \text{Balance of forces} \end{cases}$$

Coupling conditions

$$\begin{cases} \mathbf{v}^s \cdot \mathbf{n}_\Gamma = \mathbf{v}^F \cdot \mathbf{n}_\Gamma & \blacktriangleright \text{Balance of mass + Non-penetration condition} \\ (\mathcal{C}:\boldsymbol{\varepsilon}) \cdot \mathbf{n}_\Gamma = p \mathbf{n}_\Gamma & \blacktriangleright \text{Balance of forces} \end{cases}$$

Initial and boundary conditions

- Initial conditions on (ρ^s, \mathbf{v}^s) and (ρ^F, \mathbf{v}^F)
- Homogeneous Dirichlet boundary conditions on $\partial\Omega$ for simplicity

Table of Contents

1 Introduction

- Context
- DG and HHO methods
- Model Problem

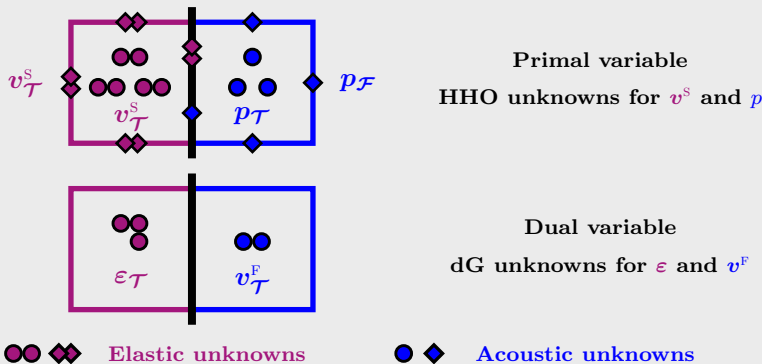
2 RK-HHO discretization

- HHO space semi-discretization
- Singly diagonally implicit RK schemes
- Explicit RK schemes

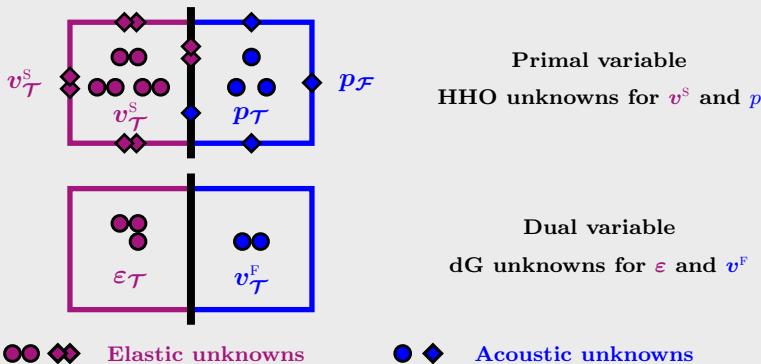
3 Numerical results

- Convergence rates
- CFL stability condition
- Ricker wavelet
- Sedimentary basin

Space semi-discretization

Fig. 6: Elasto-acoustic unknowns with $k' = 1$ and $k = 0$.

Space semi-discretization

Fig. 6: Elasto-acoustic unknowns with $k' = 1$ and $k = 0$.

References

- Same discretization as for acoustic [Burman, Duran, and Ern, 2022] and elastic [Burman, Duran, Ern, and Steins, 2021] problems, but **with coupling terms**

Local reconstruction operators

■ **Strain reconstruction:** $\mathbf{E}_T(\hat{\mathbf{v}}_T^s) : \mathbb{P}^{k'}(T, \mathbb{R}^d) \times \mathbb{P}^k(\partial T, \mathbb{R}^d) \longrightarrow \mathbb{P}^k(T; \mathbb{R}_{\text{sym}}^{d \times d})$ s.t.

$$(\mathbf{E}_T(\hat{\mathbf{v}}_T^s), \zeta)_T = (\nabla_s \mathbf{v}_T^s, \zeta)_T - (\mathbf{v}_T^s - \mathbf{v}_{\partial T}, \zeta \cdot \mathbf{n}_T)_{\partial T}, \quad \forall \zeta \in \mathbb{P}^k(T; \mathbb{R}_{\text{sym}}^{d \times d})$$

■ **Gradient reconstruction:** $\mathbf{G}_T(\hat{p}_T) : \mathbb{P}^{k'}(T, \mathbb{R}) \times \mathbb{P}^k(\partial T, \mathbb{R}) \longrightarrow \mathbb{P}^k(T; \mathbb{R}^d)$ s.t.

$$(\mathbf{G}_T(\hat{p}_T), \mathbf{q})_T = (\nabla p_T, \mathbf{q})_T - (p_T - p_{\partial T}, \mathbf{q} \cdot \mathbf{n}_T)_{\partial T}, \quad \forall \mathbf{q} \in \mathbb{P}^k(T; \mathbb{R}^d)$$

Local reconstruction operators

■ **Strain reconstruction:** $\mathbf{E}_T(\hat{\mathbf{v}}_T^s) : \mathbb{P}^{k'}(T, \mathbb{R}^d) \times \mathbb{P}^k(\partial T, \mathbb{R}^d) \longrightarrow \mathbb{P}^k(T; \mathbb{R}_{\text{sym}}^{d \times d})$ s.t.

$$(\mathbf{E}_T(\hat{\mathbf{v}}_T^s), \zeta)_T = (\nabla_s \mathbf{v}_T^s, \zeta)_T - (\mathbf{v}_T^s - \mathbf{v}_{\partial T}^s, \zeta \cdot \mathbf{n}_T)_{\partial T}, \quad \forall \zeta \in \mathbb{P}^k(T; \mathbb{R}_{\text{sym}}^{d \times d})$$

■ **Gradient reconstruction:** $\mathbf{G}_T(\hat{p}_T) : \mathbb{P}^{k'}(T, \mathbb{R}) \times \mathbb{P}^k(\partial T, \mathbb{R}) \longrightarrow \mathbb{P}^k(T; \mathbb{R}^d)$ s.t.

$$(\mathbf{G}_T(\hat{p}_T), \mathbf{q})_T = (\nabla p_T, \mathbf{q})_T - (p_T - p_{\partial T}, \mathbf{q} \cdot \mathbf{n}_T)_{\partial T}, \quad \forall \mathbf{q} \in \mathbb{P}^k(T; \mathbb{R}^d)$$

Local stabilization operators

■ **Mixed-order discretization: Stabilization in HDG** (Lehrenfeld-Schöberl)

$$S_{\partial T}(\hat{p}_T) := \Pi_{\partial T}^k(p_T - p_{\partial T}) \quad \mathbf{S}_{\partial T}(\hat{\mathbf{v}}_T^s) := \boldsymbol{\Pi}_{\partial T}^k(\mathbf{v}_T^s - \mathbf{v}_{\partial T}^s)$$

■ **Equal-order discretization: Specific stabilization to HHO**

- ▶ Needs additional velocity and pressure reconstructions

HHO space semi-discretization for the elasto-acoustic coupling

- Elastic wave equation: $\mathbf{E}_T(\hat{\mathbf{v}}_h^s)|_T := \mathbf{E}_T(\hat{\mathbf{v}}_T^s)$

$$(\partial_t \boldsymbol{\varepsilon}_T(t), \mathbf{z}_T)_{\Omega^s} - (\mathbf{E}_T(\hat{\mathbf{v}}_h^s(t)), \mathbf{z}_T)_{\Omega^s} = 0$$

$$(\rho^s \partial_t \mathbf{v}_{T^s}(t), \mathbf{w}_T)_{\Omega^s} + (\mathcal{C} : \boldsymbol{\varepsilon}_T, \mathbf{E}_T(\hat{\mathbf{w}}_h))_{\Omega^s} + s_h^s(\hat{\mathbf{v}}_h^s, \hat{\mathbf{w}}_h) + (\mathbf{p}_F(t), \mathbf{w}_F \cdot \mathbf{n}_\Gamma)_\Gamma = (\mathbf{f}^s(t), \mathbf{w}_T)_{\Omega^s}$$

- Acoustic wave equation: $\mathbf{G}_T(\hat{p}_h)|_T := \mathbf{G}_T(\hat{p}_T)$

$$(\rho^F \partial_t \mathbf{v}^F t(t), \mathbf{r}_T)_{\Omega^F} + (\mathbf{G}_T(\hat{p}_h(t)), \mathbf{r}_T)_{\Omega^F} = 0$$

$$\left(\frac{1}{\kappa} \partial_t p_T(t), q_T \right)_{\Omega^F} - (\mathbf{v}^F t(t), \mathbf{G}_T(\hat{q}_h))_{\Omega^F} + s_h^F(\hat{p}_h(t), \hat{q}_h) - (\mathbf{v}^F s(t) \cdot \mathbf{n}_\Gamma, q_F)_\Gamma = (f^F(t), q_T)_{\Omega^F}$$

HHO space semi-discretization for the elasto-acoustic coupling

- Elastic wave equation: $\mathbf{E}_T(\hat{\mathbf{v}}_h^s)|_T := \mathbf{E}_T(\hat{\mathbf{v}}_T^s)$

$$(\partial_t \boldsymbol{\varepsilon}_T(t), \mathbf{z}_T)_{\Omega^s} - (\mathbf{E}_T(\hat{\mathbf{v}}_h^s(t)), \mathbf{z}_T)_{\Omega^s} = 0$$

$$(\rho^s \partial_t \mathbf{v}_{T^s}(t), \mathbf{w}_T)_{\Omega^s} + (\mathcal{C} : \boldsymbol{\varepsilon}_T, \mathbf{E}_T(\hat{\mathbf{w}}_h))_{\Omega^s} + s_h^s(\hat{\mathbf{v}}_h^s, \hat{\mathbf{w}}_h) + (\mathbf{p}_F(t), \mathbf{w}_F \cdot \mathbf{n}_\Gamma)_\Gamma = (\mathbf{f}^s(t), \mathbf{w}_T)_{\Omega^s}$$

- Acoustic wave equation: $\mathbf{G}_T(\hat{p}_h)|_T := \mathbf{G}_T(\hat{p}_T)$

$$(\rho^F \partial_t \mathbf{v}^F t(t), \mathbf{r}_T)_{\Omega^F} + (\mathbf{G}_T(\hat{p}_h(t)), \mathbf{r}_T)_{\Omega^F} = 0$$

$$\left(\frac{1}{\kappa} \partial_t p_T(t), q_T \right)_{\Omega^F} - (\mathbf{v}^F t(t), \mathbf{G}_T(\hat{q}_h))_{\Omega^F} + s_h^F(\hat{p}_h(t), \hat{q}_h) - (\mathbf{v}^F s(t) \cdot \mathbf{n}_\Gamma, q_F)_\Gamma = (f^F(t), q_T)_{\Omega^F}$$

Global stabilization forms

$$s_h^s(\hat{\mathbf{v}}_h^s, \hat{\boldsymbol{\zeta}}_h) = \sum_{T \in \mathcal{T}_h} \tau_T^s(\mathbf{S}_{\partial T}(\hat{\mathbf{v}}_T^s), \mathbf{S}_{\partial T}(\hat{\boldsymbol{\zeta}}_T))_{\partial T}$$

$$s_h^F(\hat{p}_h, \hat{q}_h) = \sum_{T \in \mathcal{T}_h} \tau_T^F(\mathbf{S}_{\partial T}(\hat{p}_T), \mathbf{S}_{\partial T}(\hat{q}_T))_{\partial T}$$

- **with two strategies:** $\tau_T^s = \mathcal{O}(1) = \tau_T^F$ or $\tau_T^s = \mathcal{O}(1/h) = \tau_T^F$

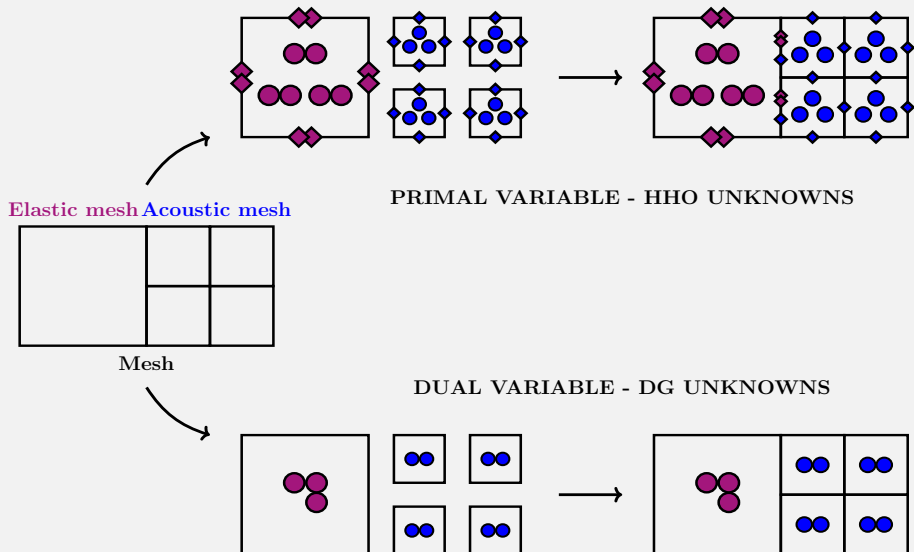


Fig. 7: Assembly procedure for the coupling in first order formulation

Algebraic realization

- Static coupling between cell and face unknowns

$$\begin{bmatrix}
 \mathbf{M}_{\mathcal{T}\mathcal{T}}^{v^F} & 0 & 0 & 0 & 0 & 0 \\
 0 & \mathbf{M}_{\mathcal{T}\mathcal{T}}^F & 0 & 0 & 0 & 0 \\
 0 & 0 & 0 & 0 & 0 & 0 \\
 \hline
 0 & 0 & 0 & \mathbf{M}_{\mathcal{T}\mathcal{T}}^e & 0 & 0 \\
 0 & 0 & 0 & 0 & \mathbf{M}_{\mathcal{T}\mathcal{T}}^s & 0 \\
 0 & 0 & 0 & 0 & 0 & 0
 \end{bmatrix} \frac{d}{dt} \begin{bmatrix}
 \mathbf{V}_{\mathcal{T}^F}^F \\
 \mathbf{P}_{\mathcal{T}^F} \\
 \mathbf{P}_{\mathcal{F}^F} \\
 \hline
 \mathbf{S}_{\mathcal{T}^s} \\
 \mathbf{V}_{\mathcal{T}^s}^s \\
 \mathbf{V}_{\mathcal{F}^s}^s
 \end{bmatrix} + \begin{bmatrix}
 0 & -G_{\mathcal{T}} & -G_{\mathcal{F}} & 0 & 0 & 0 \\
 G_{\mathcal{T}}^\dagger & \Sigma_{\mathcal{T}\mathcal{T}}^F & \Sigma_{\mathcal{T}\mathcal{F}}^F & 0 & 0 & 0 \\
 G_{\mathcal{F}}^\dagger & \Sigma_{\mathcal{F}\mathcal{T}}^F & \Sigma_{\mathcal{F}\mathcal{F}}^F & 0 & 0 & C_F \\
 0 & 0 & 0 & 0 & -E_{\mathcal{T}} & -E_{\mathcal{F}} \\
 0 & 0 & 0 & E_{\mathcal{T}}^\dagger & \Sigma_{\mathcal{T}\mathcal{T}}^S & \Sigma_{\mathcal{T}\mathcal{F}}^S \\
 0 & 0 & 0 & E_{\mathcal{F}}^\dagger & \Sigma_{\mathcal{F}\mathcal{T}}^S & \Sigma_{\mathcal{F}\mathcal{F}}^S
 \end{bmatrix} \begin{bmatrix}
 \mathbf{V}_{\mathcal{T}^F}^F \\
 \mathbf{P}_{\mathcal{T}^F} \\
 \mathbf{P}_{\mathcal{F}^F} \\
 \hline
 \mathbf{S}_{\mathcal{T}^s} \\
 \mathbf{V}_{\mathcal{T}^s}^s \\
 \mathbf{V}_{\mathcal{F}^s}^s
 \end{bmatrix} = \begin{bmatrix}
 0 \\
 \mathbf{F}_{\mathcal{T}^F}^F \\
 0 \\
 0 \\
 \mathbf{F}_{\mathcal{T}^s}^s \\
 0
 \end{bmatrix}$$

Algebraic realization

- Static coupling between cell and face unknowns

$$\left[\begin{array}{ccc|cc} \mathbf{M}_{TT}^{v^F} & 0 & 0 & 0 & 0 \\ 0 & \mathbf{M}_{TT}^F & 0 & 0 & 0 \\ 0 & 0 & 0 & 0 & 0 \\ \hline 0 & 0 & 0 & \mathbf{M}_{TT}^{\epsilon} & 0 & 0 \\ 0 & 0 & 0 & 0 & \mathbf{M}_{TT}^S & 0 \\ 0 & 0 & 0 & 0 & 0 & 0 \end{array} \right] \frac{d}{dt} \begin{bmatrix} \mathbf{V}_{T^F}^F \\ \mathbf{P}_{T^F} \\ \mathbf{P}_{F^F} \\ \mathbf{S}_{T^S} \\ \mathbf{V}_{T^S}^S \\ \mathbf{V}_{F^S}^S \end{bmatrix} + \begin{bmatrix} 0 & -G_T & -G_F & 0 & 0 & 0 \\ G_T^\dagger & \Sigma_{TT}^F & \Sigma_{TF}^F & 0 & 0 & 0 \\ G_F^\dagger & \Sigma_{FT}^F & \Sigma_{FF}^F & 0 & 0 & C_R \\ 0 & 0 & 0 & 0 & -E_T & -E_F \\ 0 & 0 & 0 & E_T^\dagger & \Sigma_{TT}^S & \Sigma_{TF}^S \\ 0 & 0 & 0 & E_F^\dagger & \Sigma_{FT}^S & \Sigma_{FF}^S \end{bmatrix} \begin{bmatrix} \mathbf{V}_{T^F}^F \\ \mathbf{P}_{T^F} \\ \mathbf{P}_{F^F} \\ \mathbf{S}_{T^S} \\ \mathbf{V}_{T^S}^S \\ \mathbf{V}_{F^S}^S \end{bmatrix} = \begin{bmatrix} 0 \\ \mathbf{F}_{T^F}^F \\ 0 \\ 0 \\ \mathbf{F}_{T^S}^S \\ 0 \end{bmatrix}$$

- Rearrangement of dofs: cell unknowns first and then face unknowns

$$\left[\begin{array}{ccc|cc} \mathbf{M}_{TT}^{v^F} & 0 & 0 & 0 & 0 \\ 0 & \mathbf{M}_{TT}^F & 0 & 0 & 0 \\ 0 & 0 & \mathbf{M}_{TT}^{\epsilon} & 0 & 0 \\ 0 & 0 & 0 & \mathbf{M}_{TT}^S & 0 & 0 \\ 0 & 0 & 0 & 0 & 0 & 0 \\ 0 & 0 & 0 & 0 & 0 & 0 \end{array} \right] \frac{d}{dt} \begin{bmatrix} \mathbf{V}_{T^F}^F \\ \mathbf{P}_{T^F} \\ \mathbf{S}_{T^S} \\ \mathbf{V}_{T^S}^S \\ \mathbf{P}_{F^F} \\ \mathbf{V}_{F^S}^S \end{bmatrix} + \begin{bmatrix} 0 & -G_T & 0 & 0 & -G_F & 0 \\ G_T^\dagger & \Sigma_{TT}^F & 0 & 0 & \Sigma_{TF}^F & 0 \\ 0 & 0 & 0 & -E_T & 0 & -E_F \\ 0 & 0 & E_T^\dagger & \Sigma_{TT}^S & 0 & \Sigma_{TF}^S \\ G_F^\dagger & \Sigma_{FT}^F & 0 & 0 & \Sigma_{FF}^F & C_R \\ 0 & 0 & E_F^\dagger & \Sigma_{FT}^S & -C_R^\dagger & \Sigma_{FF}^S \end{bmatrix} \begin{bmatrix} \mathbf{V}_{T^F}^F \\ \mathbf{P}_{T^F} \\ \mathbf{S}_{T^S} \\ \mathbf{V}_{T^S}^S \\ \mathbf{P}_{F^F} \\ \mathbf{V}_{F^S}^S \end{bmatrix} = \begin{bmatrix} 0 \\ \mathbf{F}_{T^F}^F \\ 0 \\ 0 \\ \mathbf{F}_{T^S}^S \\ 0 \end{bmatrix}$$

SDIRK(s, s + 1) schemes

- Generic ODE with $f : J \times \mathbb{R}^m \rightarrow \mathbb{R}^m$,

$$\begin{cases} y'(t) = f(t, y(t)), & \forall t \in J := [0, T] \\ y|_{t=0} = y_0 \in \mathbb{R}^m \end{cases}$$

SDIRK($s, s + 1$) schemes

- Generic ODE with $f : J \times \mathbb{R}^m \rightarrow \mathbb{R}^m$,

$$\begin{cases} y'(t) = f(t, y(t)), & \forall t \in J := [0, T] \\ y|_{t=0} = y_0 \in \mathbb{R}^m \end{cases}$$

- SDIRK($s, s + 1$) consists

- ▶ in solving sequentially for all $i \in \{1, \dots, s\}$,

$$u_{\textcolor{red}{i}}^{[n]} = u_{n-1} + \Delta t \sum_{j=1}^{\textcolor{red}{i}} a_{ij} f(t_{n-1} + c_j \Delta t, u_j^{[n]})$$

- ▶ and setting

$$u_n := u_{n-1} + \Delta t \sum_{j=1}^s b_j f(t_{n-1} + c_j \Delta t, u_j^{[n]})$$

c_1	$\textcolor{red}{a}_*$	0	\cdots	0
c_2	a_{21}	$\textcolor{red}{a}_*$	\ddots	0
\vdots	\vdots	\ddots	\ddots	\vdots
c_s	a_{s1}	\cdots	$a_{s,s-1}$	$\textcolor{red}{a}_*$

Algebraic realization of SDIRK-HHO

- Face-based sparse linear system to be solved at each stage
- We solve sequentially for all $i \in \{1, \dots, s\}$,

$$\left[\begin{array}{c|cc|cc} \mathbf{M}_{TT}^{v^F} & 0 & 0 & 0 & 0 \\ \hline 0 & \mathbf{M}_{TT}^F & 0 & 0 & 0 \\ \hline 0 & 0 & \mathbf{M}_{TT}^{\epsilon} & 0 & 0 \\ \hline 0 & 0 & 0 & \mathbf{M}_{TT}^S & 0 \\ \hline 0 & 0 & 0 & 0 & 0 \\ \hline 0 & 0 & 0 & 0 & 0 \end{array} \right] \left[\begin{array}{c} \mathbf{V}_{T^F}^{F,n,i} \\ \mathbf{P}_{T^F}^{n,i} \\ \mathbf{S}_{T^S}^{n,i} \\ \mathbf{V}_{T^S}^{S,n,i} \\ \mathbf{P}_{T^S}^{n,i} \\ \mathbf{V}_{T^S}^{S,n,i} \end{array} \right] = \left[\begin{array}{c|cc|cc} \mathbf{M}_{TT}^{v^F} & 0 & 0 & 0 & 0 \\ \hline 0 & \mathbf{M}_{TT}^F & 0 & 0 & 0 \\ \hline 0 & 0 & \mathbf{M}_{TT}^{\epsilon} & 0 & 0 \\ \hline 0 & 0 & 0 & \mathbf{M}_{TT}^S & 0 \\ \hline 0 & 0 & 0 & 0 & 0 \\ \hline 0 & 0 & 0 & 0 & 0 \end{array} \right] \left[\begin{array}{c} \mathbf{V}_{T^F}^{F,n-1} \\ \mathbf{P}_{T^F}^{n-1} \\ \mathbf{S}_{T^S}^{n-1} \\ \mathbf{V}_{T^S}^{S,n-1} \\ \mathbf{P}_{T^S}^{n-1} \\ \mathbf{V}_{T^S}^{S,n-1} \end{array} \right]$$

$$+ \Delta t \sum_{j=1}^i a_{ij} \left(\left[\begin{array}{c} 0 \\ F_{T^F}^{F,n-1+c_j} \\ 0 \\ F_{T^F}^{S,n-1+c_j} \\ 0 \\ 0 \end{array} \right] - \left[\begin{array}{c|cc|cc} 0 & -G_T & 0 & 0 & -G_F & 0 \\ \hline G_T^\dagger & \Sigma_{TT}^F & 0 & 0 & \Sigma_{TF}^F & 0 \\ \hline 0 & 0 & 0 & -E_T & 0 & -E_F \\ \hline 0 & 0 & E_T^\dagger & \Sigma_{TT}^S & 0 & \Sigma_{TF}^S \\ \hline G_F^\dagger & \Sigma_{FT}^F & 0 & 0 & \Sigma_{FF}^F & C^F \\ \hline 0 & 0 & E_F^\dagger & \Sigma_{FT}^S & -C_\Gamma^\dagger & \Sigma_{FF}^S \end{array} \right] \right)$$

Algebraic realization of SDIRK-HHO

- Face-based sparse linear system to be solved at each stage
- We solve sequentially for all $i \in \{1, \dots, s\}$,

$$\left[\begin{array}{c|cc|cc} \mathbf{M}_{TT}^{v^F} & 0 & 0 & 0 & 0 \\ \hline 0 & \mathbf{M}_{TT}^F & 0 & 0 & 0 \\ \hline 0 & 0 & \mathbf{M}_{TT}^e & 0 & 0 \\ \hline 0 & 0 & 0 & \mathbf{M}_{TT}^s & 0 \\ \hline 0 & 0 & 0 & 0 & 0 \\ \hline 0 & 0 & 0 & 0 & 0 \end{array} \right] \left[\begin{array}{c} \mathbf{V}_{T^F}^{F,n,i} \\ \mathbf{P}_{T^F}^{n,i} \\ \mathbf{S}_{T^s}^{n,i} \\ \mathbf{V}_{T^s}^{S,n,i} \\ \mathbf{P}_{T^s}^{n,i} \\ \mathbf{V}_{T^s}^{S,n,i} \end{array} \right] = \left[\begin{array}{c|cc|cc} \mathbf{M}_{TT}^{v^F} & 0 & 0 & 0 & 0 \\ \hline 0 & \mathbf{M}_{TT}^F & 0 & 0 & 0 \\ \hline 0 & 0 & \mathbf{M}_{TT}^e & 0 & 0 \\ \hline 0 & 0 & 0 & \mathbf{M}_{TT}^s & 0 \\ \hline 0 & 0 & 0 & 0 & 0 \\ \hline 0 & 0 & 0 & 0 & 0 \end{array} \right] \left[\begin{array}{c} \mathbf{V}_{T^F}^{F,n-1} \\ \mathbf{P}_{T^F}^{n-1} \\ \mathbf{S}_{T^s}^{n-1} \\ \mathbf{V}_{T^s}^{S,n-1} \\ \mathbf{P}_{T^s}^{n-1} \\ \mathbf{V}_{T^s}^{S,n-1} \end{array} \right]$$

$$+ \Delta t \sum_{j=1}^i a_{ij} \left(\left[\begin{array}{c} 0 \\ F_{T^F}^{F,n-1+c_j} \\ 0 \\ F_{T^F}^{S,n-1+c_j} \\ 0 \\ 0 \end{array} \right] - \left[\begin{array}{c|cc|cc} 0 & -G_T & 0 & 0 & -G_F & 0 \\ \hline G_T^\dagger & \Sigma_{TT}^F & 0 & 0 & \Sigma_{TF}^F & 0 \\ \hline 0 & 0 & 0 & -E_T & 0 & -E_F \\ \hline 0 & 0 & E_T^\dagger & \Sigma_{TT}^S & 0 & \Sigma_{TF}^S \\ \hline G_F^\dagger & \Sigma_{FT}^F & 0 & 0 & \Sigma_{FF}^F & C^F \\ \hline 0 & 0 & E_F^\dagger & \Sigma_{FT}^S & -C_\Gamma^\dagger & \Sigma_{FF}^S \end{array} \right] \right)$$

- The upper 4×4 submatrix associated with all the cell unknowns is block-diagonal
 - Schur complement procedure

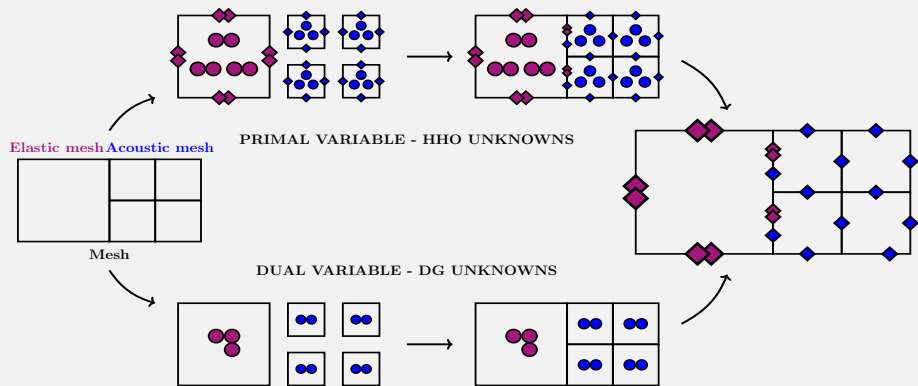


Fig. 8: Assembly and static condensation procedure for the coupling in first order formulation

ERK(s) schemes

- ERK(s) consists

- ▶ in updating sequentially for all $i \in \{1, \dots, s\}$,

$$u_i^{[n]} = u_{n-1} + \Delta t \sum_{j=1}^{i-1} a_{ij} f(t_{n-1} + c_j \Delta t, u_j^{[n]})$$

- ▶ and setting

$$u_n := u_{n-1} + \Delta t \sum_{j=1}^s b_j f\left(t_{n-1} + c_j \Delta t, u_j^{[n]}\right)$$

c_1	0	\cdots	\cdots	0
c_2	a_{21}	0	\cdots	0
\vdots	\vdots	\ddots	\ddots	\vdots
c_s	a_{s1}	\cdots	$a_{s,s-1}$	0
	b_1	\cdots	b_{s-1}	b_s

HHO-ERK scheme

- Coupling of face unknowns at the interface Γ

$$\left[\begin{array}{cc|cc|cc} \mathbf{M}_{\mathcal{T}\mathcal{T}}^{\mathcal{F}} & 0 & 0 & 0 & 0 & 0 \\ 0 & \mathbf{M}_{\mathcal{T}\mathcal{T}}^{\mathcal{F}} & 0 & 0 & 0 & 0 \\ \hline 0 & 0 & \mathbf{M}_{\mathcal{T}\mathcal{T}}^{\mathcal{E}} & 0 & 0 & 0 \\ 0 & 0 & 0 & \mathbf{M}_{\mathcal{T}\mathcal{T}}^{\mathcal{S}} & 0 & 0 \\ \hline 0 & 0 & 0 & 0 & 0 & 0 \\ 0 & 0 & 0 & 0 & 0 & 0 \end{array} \right] \left[\begin{array}{c} \mathbf{V}_{\mathcal{T}^{\mathcal{F}}}^{\mathcal{F},n,i} \\ \mathbf{P}_{\mathcal{T}^{\mathcal{F}}}^{n,i} \\ \hline \mathbf{S}_{\mathcal{T}^{\mathcal{s}}}^{n,i} \\ \mathbf{V}_{\mathcal{T}^{\mathcal{s}}}^{s,n,i} \\ \mathbf{P}_{\mathcal{F}^{\mathcal{F}}}^{n,i} \\ \mathbf{V}_{\mathcal{F}^{\mathcal{F}}}^{s,n,i} \end{array} \right] = \left[\begin{array}{cc|cc|cc} \mathbf{M}_{\mathcal{T}\mathcal{T}}^{\mathcal{F}} & 0 & 0 & 0 & 0 & 0 \\ 0 & \mathbf{M}_{\mathcal{T}\mathcal{T}}^{\mathcal{F}} & 0 & 0 & 0 & 0 \\ \hline 0 & 0 & \mathbf{M}_{\mathcal{T}\mathcal{T}}^{\mathcal{E}} & 0 & 0 & 0 \\ 0 & 0 & 0 & \mathbf{M}_{\mathcal{T}\mathcal{T}}^{\mathcal{S}} & 0 & 0 \\ \hline 0 & 0 & 0 & 0 & 0 & 0 \\ 0 & 0 & 0 & 0 & 0 & 0 \end{array} \right] \left[\begin{array}{c} \mathbf{V}_{\mathcal{T}^{\mathcal{F}}}^{\mathcal{F},n-1} \\ \mathbf{P}_{\mathcal{T}^{\mathcal{F}}}^{n-1} \\ \hline \mathbf{S}_{\mathcal{T}^{\mathcal{s}}}^{n-1} \\ \mathbf{V}_{\mathcal{T}^{\mathcal{s}}}^{s,n-1} \\ \mathbf{P}_{\mathcal{F}^{\mathcal{F}}}^{n-1} \\ \mathbf{V}_{\mathcal{F}^{\mathcal{F}}}^{s,n-1} \end{array} \right]$$

$$+ \Delta t \sum_{j=1}^{i-1} a_{ij} \left(\left[\begin{array}{c} 0 \\ F_{\mathcal{T}^{\mathcal{F}}}^{\mathcal{F},n-1+c_j} \\ \hline 0 \\ F_{\mathcal{T}^{\mathcal{s}}}^{s,n-1+c_j} \\ \hline 0 \\ 0 \end{array} \right] - \left[\begin{array}{cc|cc|cc} 0 & -G_{\mathcal{T}} & 0 & 0 & -G_{\mathcal{F}} & 0 \\ G_{\mathcal{T}}^\dagger & \Sigma_{\mathcal{T}\mathcal{T}}^{\mathcal{F}} & 0 & 0 & \Sigma_{\mathcal{T}\mathcal{F}}^{\mathcal{F}} & 0 \\ \hline 0 & 0 & 0 & -E_{\mathcal{T}} & 0 & -E_{\mathcal{F}} \\ 0 & 0 & E_{\mathcal{T}}^\dagger & \Sigma_{\mathcal{T}\mathcal{T}}^{\mathcal{S}} & 0 & \Sigma_{\mathcal{T}\mathcal{F}}^{\mathcal{S}} \\ \hline G_{\mathcal{F}}^\dagger & \Sigma_{\mathcal{F}\mathcal{T}}^{\mathcal{F}} & 0 & 0 & \Sigma_{\mathcal{F}\mathcal{F}}^{\mathcal{F}} & C^{\mathcal{F}} \\ 0 & 0 & E_{\mathcal{F}}^\dagger & \Sigma_{\mathcal{F}\mathcal{T}}^{\mathcal{S}} & -C_{\mathcal{T}}^\dagger & \Sigma_{\mathcal{F}\mathcal{F}}^{\mathcal{S}} \end{array} \right] \left[\begin{array}{c} \mathbf{V}_{\mathcal{T}^{\mathcal{F}}}^{\mathcal{F},n,j} \\ \mathbf{P}_{\mathcal{T}^{\mathcal{F}}}^{n,j} \\ \hline \mathbf{S}_{\mathcal{T}^{\mathcal{s}}}^{n,j} \\ \mathbf{V}_{\mathcal{T}^{\mathcal{s}}}^{s,n,j} \\ \mathbf{P}_{\mathcal{F}^{\mathcal{F}}}^{n,j} \\ \mathbf{V}_{\mathcal{F}^{\mathcal{F}}}^{s,n,j} \end{array} \right] \right)$$

HHO-ERK scheme

- Coupling of face unknowns at the interface Γ

$$\left[\begin{array}{c|cc|cc} \mathbf{M}_{\mathcal{T}\mathcal{T}}^{v^F} & 0 & 0 & 0 & 0 \\ \hline 0 & \mathbf{M}_{\mathcal{T}\mathcal{T}}^F & 0 & 0 & 0 \\ \hline 0 & 0 & \mathbf{M}_{\mathcal{T}\mathcal{T}}^{\epsilon} & 0 & 0 \\ 0 & 0 & 0 & \mathbf{M}_{\mathcal{T}\mathcal{T}}^S & 0 \\ \hline 0 & 0 & 0 & 0 & 0 \\ 0 & 0 & 0 & 0 & 0 \end{array} \right] \left[\begin{array}{c} \mathbf{V}_{\mathcal{T}^F}^{F,n,i} \\ \mathbf{P}_{\mathcal{T}^F}^{n,i} \\ \hline \mathbf{S}_{\mathcal{T}^s}^{n,i} \\ \mathbf{V}_{\mathcal{T}^s}^{S,n,i} \\ \mathbf{P}_{\mathcal{F}^F}^{n,i} \\ \mathbf{V}_{\mathcal{F}^s}^{S,n,i} \end{array} \right] = \left[\begin{array}{c|cc|cc} \mathbf{M}_{\mathcal{T}\mathcal{T}}^{v^F} & 0 & 0 & 0 & 0 \\ \hline 0 & \mathbf{M}_{\mathcal{T}\mathcal{T}}^F & 0 & 0 & 0 \\ \hline 0 & 0 & \mathbf{M}_{\mathcal{T}\mathcal{T}}^{\epsilon} & 0 & 0 \\ 0 & 0 & 0 & \mathbf{M}_{\mathcal{T}\mathcal{T}}^S & 0 \\ \hline 0 & 0 & 0 & 0 & 0 \\ 0 & 0 & 0 & 0 & 0 \end{array} \right] \left[\begin{array}{c} \mathbf{V}_{\mathcal{T}^F}^{F,n-1} \\ \mathbf{P}_{\mathcal{T}^F}^{n-1} \\ \hline \mathbf{S}_{\mathcal{T}^s}^{n-1} \\ \mathbf{V}_{\mathcal{T}^s}^{S,n-1} \\ \mathbf{P}_{\mathcal{F}^F}^{n-1} \\ \mathbf{V}_{\mathcal{F}^s}^{S,n-1} \end{array} \right]$$

$$+ \Delta t \sum_{j=1}^{i-1} a_{ij} \left(\left[\begin{array}{c} 0 \\ F_{\mathcal{T}^F}^{F,n-1+c_j} \\ \hline 0 \\ F_{\mathcal{T}^s}^{S,n-1+c_j} \\ \hline 0 \\ 0 \end{array} \right] - \left[\begin{array}{c|cc|cc} 0 & -G_{\mathcal{T}} & 0 & 0 & -G_{\mathcal{F}} & 0 \\ G_{\mathcal{T}}^\dagger & \Sigma_{\mathcal{T}\mathcal{T}}^F & 0 & 0 & \Sigma_{\mathcal{T}\mathcal{F}}^F & 0 \\ \hline 0 & 0 & 0 & -E_{\mathcal{T}} & 0 & -E_{\mathcal{F}} \\ 0 & 0 & E_{\mathcal{T}}^\dagger & \Sigma_{\mathcal{T}\mathcal{T}}^S & 0 & \Sigma_{\mathcal{T}\mathcal{F}}^S \\ G_{\mathcal{F}}^\dagger & \Sigma_{\mathcal{F}\mathcal{T}}^F & 0 & 0 & \Sigma_{\mathcal{F}\mathcal{F}}^F & C^F \\ 0 & 0 & E_{\mathcal{F}}^\dagger & \Sigma_{\mathcal{F}\mathcal{T}}^S & -C_\Gamma^\dagger & \Sigma_{\mathcal{F}\mathcal{F}}^S \end{array} \right] \left[\begin{array}{c} \mathbf{V}_{\mathcal{T}^F}^{F,n,j} \\ \mathbf{P}_{\mathcal{T}^F}^{n,j} \\ \hline \mathbf{S}_{\mathcal{T}^s}^{n,j} \\ \mathbf{V}_{\mathcal{T}^s}^{S,n,j} \\ \mathbf{P}_{\mathcal{F}^F}^{n,j} \\ \mathbf{V}_{\mathcal{F}^s}^{S,n,j} \end{array} \right] \right)$$

- Key question:** how to inverse efficiently

$$\left[\begin{array}{cc} \Sigma_{\mathcal{F}\mathcal{F}}^F & C^F \\ -C_\Gamma^\dagger & \Sigma_{\mathcal{F}\mathcal{F}}^S \end{array} \right] ?$$

Rearrangement of the face terms for the inversion of coupling block

- Distinguish between internal faces in $\Omega^S \cup \Omega^F$ and faces located on Γ

$$\begin{bmatrix} \Sigma_{FF}^F & 0 & 0 & 0 \\ 0 & \Sigma_{FF}^S & 0 & 0 \\ 0 & 0 & \Sigma_{FF}^F & C_\Gamma \\ 0 & 0 & -C_\Gamma^\dagger & \Sigma_{FF}^S \end{bmatrix} \begin{bmatrix} P_{\mathcal{F}_h^{OF}} \\ V_{\mathcal{F}_h^{OS}} \\ P_{\mathcal{F}_h^{o\Gamma}} \\ V_{\mathcal{F}_h^{o\Gamma}} \end{bmatrix} \rightarrow \begin{bmatrix} \Sigma_{F1}^F & C_{F1} & 0 & 0 & 0 & 0 \\ -C_{F1}^\dagger & \Sigma_{F1}^S & 0 & 0 & 0 & 0 \\ 0 & 0 & \ddots & & 0 & 0 \\ 0 & 0 & & \ddots & 0 & 0 \\ 0 & 0 & 0 & 0 & \Sigma_{Fn}^F & C_{Fn} \\ 0 & 0 & 0 & 0 & -C_{Fn}^\dagger & \Sigma_{Fn}^S \end{bmatrix} \begin{bmatrix} P_{Fn} \\ V_{Fn}^S \end{bmatrix}$$

- Block-diagonal structure for **mixed-order** setting

Table of Contents

- 1 Introduction
 - Context
 - DG and HHO methods
 - Model Problem
- 2 RK-HHO discretization
 - HHO space semi-discretization
 - Singly diagonally implicit RK schemes
 - Explicit RK schemes
- 3 Numerical results
 - Convergence rates
 - CFL stability condition
 - Ricker wavelet
 - Sedimentary basin

Computational parameters

- Space refinement: $h = 0.1 \times 2^{-\ell}$ (in each subdomain)
- Time refinement: $\Delta t = 0.1 \times 2^{-n}$

Computational parameters

- Space refinement: $h = 0.1 \times 2^{-\ell}$ (in each subdomain)
- Time refinement: $\Delta t = 0.1 \times 2^{-n}$

Meshes

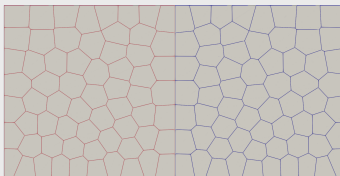
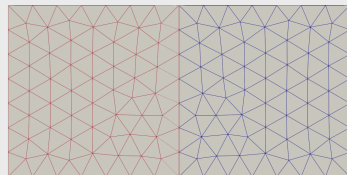
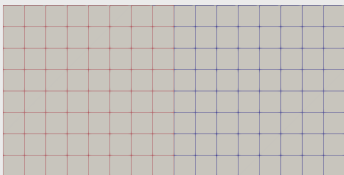


Fig. 9: Cartesian, simplicial and polyhedral meshes for $\ell = 0$

Convergence rates in space

- **Analytical solution:** polynomial in time, sinusoidal in space
- **SDIRK(3,4)-HHO scheme** ■ $n = 8$ ■ $\ell \in \{0, 1, 2, 3, 4\}$

Convergence rates in space

■ **Analytical solution:** polynomial in time, sinusoidal in space

■ **SDIRK(3,4)-HHO scheme**

■ $n = 8$

■ $\ell \in \{0, 1, 2, 3, 4\}$

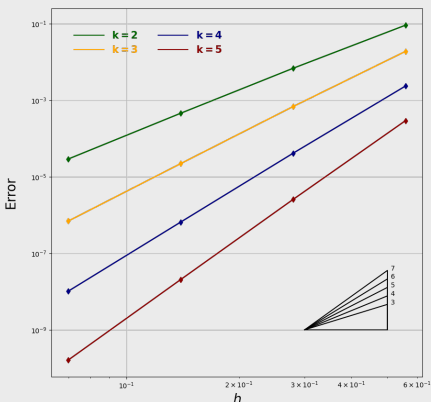
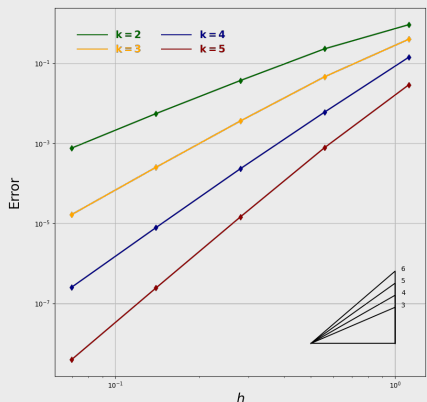


Fig. 10: L^2 -errors for the HHO-SDIRK(3,4) schemes as a function of the mesh-size. **Left:** $\tau_T^F = \mathcal{O}(1) = \tau_T^S$. **Right:** $\tau_T^F = \mathcal{O}(h_T^{-1}) = \tau_T^S$

CFL stability condition for ERK(s)-HHO

■ **CFL condition of the form** $c_{\sharp} \frac{\Delta t}{h} \leq \beta(s) \mu(k) \gamma(\eta)$

- ▶ c_{\sharp} : largest velocity in the domain
- ▶ s : number of stages
- ▶ k : polynomial order of the method
- ▶ η : stabilisation coefficient ($\tau_T^S, \tau_T^F \propto \eta$)

CFL stability condition for ERK(s)-HHO

■ **CFL condition of the form** $c_{\sharp} \frac{\Delta t}{h} \leq \beta(s) \mu(k) \gamma(\eta)$

- ▶ c_{\sharp} : largest velocity in the domain
- ▶ s : number of stages
- ▶ k : polynomial order of the method
- ▶ η : stabilisation coefficient ($\tau_T^S, \tau_T^F \propto \eta$)

$\beta(s)/\beta(4)$	η	1/8	1/4	1/2	1	2	4	8
$s = 2$		0,72	0,72	0,72	0,72	0,72	0,72	0,72
$s = 3$		0,91	0,90	0,90	0,88	0,90	0,90	0,91

Tab. 1: Study of $\beta(s)$ for $k = 1$, $\eta \in \{1/8, 1/4, \dots, 1, \dots, 4, 8\}$

CFL stability condition for ERK(s)-HHO

■ **CFL condition of the form** $c_{\sharp} \frac{\Delta t}{h} \leq \beta(s) \mu(k) \gamma(\eta)$

- ▶ c_{\sharp} : largest velocity in the domain
- ▶ s : number of stages
- ▶ k : polynomial order of the method
- ▶ η : stabilisation coefficient ($\tau_T^S, \tau_T^F \propto \eta$)

$\beta(s)/\beta(4)$	η	1/8	1/4	1/2	1	2	4	8
$s = 2$		0,72	0,72	0,72	0,72	0,72	0,72	0,72
$s = 3$		0,91	0,90	0,90	0,88	0,90	0,90	0,91

Tab. 1: Study of $\beta(s)$ for $k = 1$, $\eta \in \{1/8, 1/4, \dots, 1, \dots, 4, 8\}$

$\mu(k)/\mu(1)$	η	1/8	1/4	1/2	1	2	4	8
$k = 2$		0,48	0,48	0,46	0,59	0,64	0,63	0,64
$k = 3$		0,31	0,30	0,28	0,40	0,42	0,42	0,42

Tab. 2: Study of $\mu(k)$ for $s = 4$, $\eta \in \{1/8, 1/4, \dots, 1, \dots, 4, 8\}$

Study of $\gamma(\eta)$ on quadrangular meshes

■ **Meshes:** Quadrangular

■ **Computational parameters:**

$$k = 1, \quad s = 4$$

■ **Evolution of η as $\min(\eta, 1/\eta)$**

- ▶ Optimal CFL condition for $\eta = 1$

- ▶ Stabilisation parameters

$\tau_T^F = \mathcal{O}(h_T^{-1}) = \tau_T^S$ strongly
degrade CFL

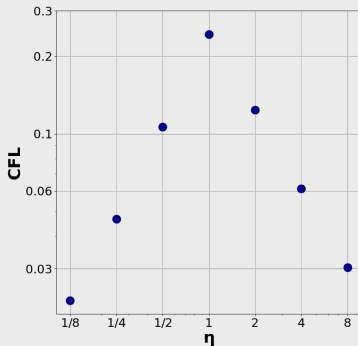


Fig. 11: CFL as a function of η

Study of $\gamma(\eta)$ on quadrangular meshes

- **Meshes:** Quadrangular

- **Computational parameters:**

$$k = 1, \quad s = 4$$

- **Evolution of η as $\min(\eta, 1/\eta)$**

- ▶ Optimal CFL condition for $\eta = 1$
- ▶ Stabilisation parameters
 $\tau_T^F = \mathcal{O}(h_T^{-1}) = \tau_T^S$ strongly
 degrade CFL

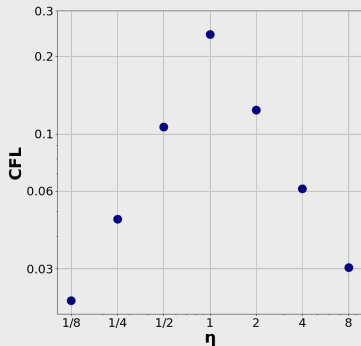


Fig. 11: CFL as a function of η

Influence of the cell geometry (simplex / quadrangle / polyhedron)

- Same conclusion for η -dependence
- **Slight CFL improvement with increase of number of faces**

Meshes	\triangle	\square	\diamond
CFL	0.2361	0.2427	0.2670
ratio	1	1.028	1.131

Tab. 3: CFL coefficient for $\eta = 1, k = 1, s = 4$

Realistic test case with strong property contrast: Granite-Water

- **Initial condition:** velocity Ricker wavelet centered at point $(x_c, y_c) \in \Omega_f$,

$$\mathbf{v}_0(x, y) := \theta e^{-\pi^2 \frac{r^2}{\lambda^2}} \begin{pmatrix} x - x_c \\ y - y_c \end{pmatrix}$$

- **Material properties:** Elastic subdomain: Granite | Acoustic subdomain: Water

Realistic test case with strong property contrast: Granite-Water

- **Initial condition:** velocity Ricker wavelet centered at point $(x_c, y_c) \in \Omega_f$,

$$\mathbf{v}_0(x, y) := \theta e^{-\pi^2 \frac{r^2}{\lambda^2}} \begin{pmatrix} x - x_c \\ y - y_c \end{pmatrix}$$

- **Material properties:** Elastic subdomain: Granite | Acoustic subdomain: Water
- **Computational parameters:** SDIRK(3,4), $n = 8$, $l = 7$, $k = 2$

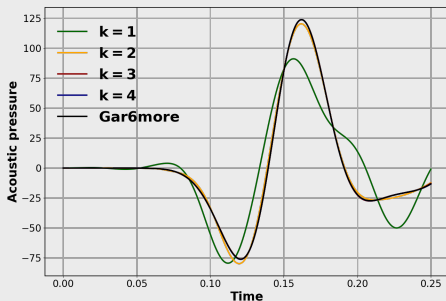
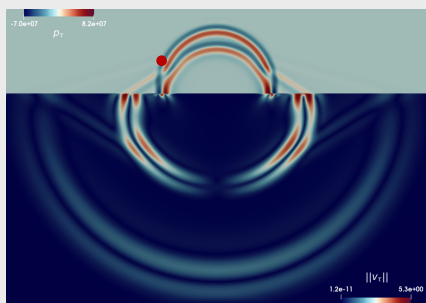


Fig. 12: Left panel: Acoustic pressure (upper side) and elastic velocity norm (lower side) at time $t = 0.375$ s. Right panel: Comparison to analytical solution (Gar6more).

Propagation of an elastic pulse in sedimentary basin and atmosphere

■ Material properties:

- ▶ **Sedimentary basin:** $\rho^S = 1200 \text{ kg.m}^{-3}$, $c_p^S = 3400 \text{ m.s}^{-1}$, $c_s = 1400 \text{ m.s}^{-1}$
- ▶ **Bedrock:** $\rho^S = 5350 \text{ kg.m}^{-3}$, $c_p^S = 3090 \text{ m.s}^{-1}$, $c_s = 2570 \text{ m.s}^{-1}$
- ▶ **Air:** $\rho^F = 1.292 \text{ kg.m}^{-3}$, $c_p^F = 340 \text{ m.s}^{-1}$

Propagation of an elastic pulse in sedimentary basin and atmosphere

■ Material properties:

- ▶ **Sedimentary basin:** $\rho^S = 1200 \text{ kg.m}^{-3}$, $c_p^S = 3400 \text{ m.s}^{-1}$, $c_s = 1400 \text{ m.s}^{-1}$
- ▶ **Bedrock:** $\rho^S = 5350 \text{ kg.m}^{-3}$, $c_p^S = 3090 \text{ m.s}^{-1}$, $c_s = 2570 \text{ m.s}^{-1}$
- ▶ **Air:** $\rho^F = 1.292 \text{ kg.m}^{-3}$, $c_p^F = 340 \text{ m.s}^{-1}$

■ Computational parameters: SDIRK(3,4), $k = 1$, $\ell = 8$, $n = 9$

■ Homogeneous Dirichlet boundary conditions

■ Initial condition: velocity Ricker wavelet centered at point $(x_c, y_c) \in \Omega_{scs}$

Propagation of an elastic pulse in sedimentary basin and atmosphere

■ Material properties:

- ▶ **Sedimentary basin:** $\rho^S = 1200 \text{ kg.m}^{-3}$, $c_p^S = 3400 \text{ m.s}^{-1}$, $c_s = 1400 \text{ m.s}^{-1}$
- ▶ **Bedrock:** $\rho^S = 5350 \text{ kg.m}^{-3}$, $c_p^S = 3090 \text{ m.s}^{-1}$, $c_s = 2570 \text{ m.s}^{-1}$
- ▶ **Air:** $\rho^F = 1.292 \text{ kg.m}^{-3}$, $c_p^F = 340 \text{ m.s}^{-1}$

■ Computational parameters:

SDIRK(3,4), $k = 1$, $\ell = 8$, $n = 9$

■ Homogeneous Dirichlet boundary conditions

■ Initial condition:

velocity Ricker wavelet centered at point $(x_c, y_c) \in \Omega_{scs}$

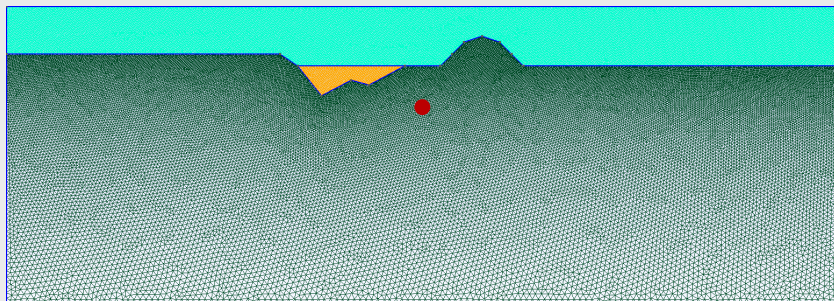


Fig. 13: Mesh of sedimentary basin

Propagation of elastic pulse in sedimentary basin and atmosphere

■ Energy transfer enhancement above sedimentary basin

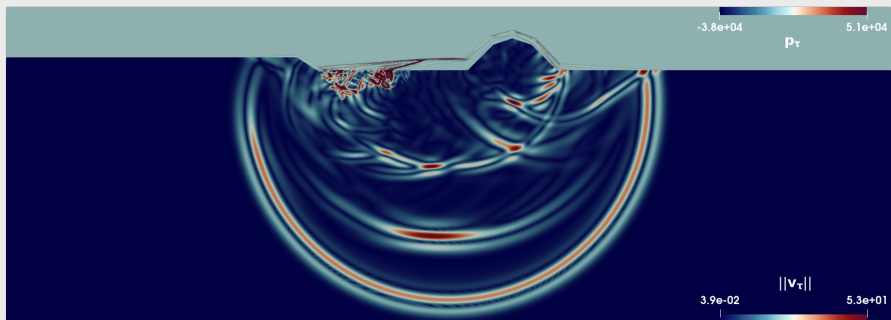


Fig. 14: Propagation of elastic pulse in sedimentary basin and atmosphere

Propagation of elastic pulse in sedimentary basin and atmosphere

■ Energy transfer enhancement above sedimentary basin

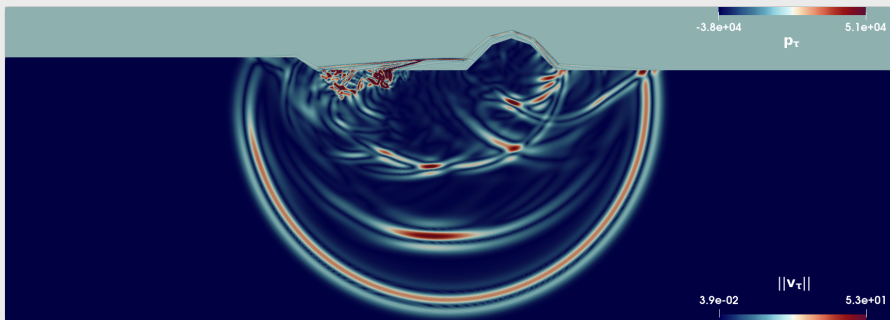


Fig. 14: Propagation of elastic pulse in sedimentary basin and atmosphere

Thank you for your attention !